A Versatile Precursor System for Supercritical Fluid Electrodeposition of Main Group Materials

Philip N. Bartlett,[a]* Jennifer Burt,[a] David A. Cook,[a] Charles Y. Cummings,[a] Michael W. George,[b],[c] Andrew L. Hector,[a] Mahboba M. Hasan,[a] Jie Ke,[b] William Levason,[a] David Pugh,[a] Gillian Reid,[a] Peter W. Richardson,[a] David C. Smith,[d] Joe Spencer,[d] Norhidayah Suleiman,[c] Wenjian Zhang[a]

Abstract

We describe a versatile electrolyte bath that can be used to electrodeposit a wide range of p-block elements from supercritical difluoromethane ($scCH_2F_2$), for the first time. The bath comprises the tetrabutylammonium chlorometallate complex of the element in an electrolyte of 50 × 10^{-3} mol dm^{-3} tetrabutylammonium chloride at 17.2 MPa and 358 K. Using the anionic ($[GaCl_4]^-$, $[InCl_4]^-$, $[GeCl_3]^-$, $[SnCl_3]^-$, $[SbCl_4]^-$, and $[BiCl_4]^-$) and dianionic ($[SeCl_6]^{2-}$ and $[TeCl_6]^{2-}$) chlorometallate salts, we demonstrate the deposition of elemental Ga, In, Ge, Sn, Sb, Bi, Se, Te. In all cases, with the exception of Ga which is a liquid under the deposition conditions, the resulting deposits are characterised by scanning electron microscopy, energy dispersive X-ray analysis, X-ray diffraction and Raman spectroscopy. An advantage of this electrolyte system is that the reagents are all crystalline solids that are reasonably easy to handle and that are not highly water or oxygen sensitive. The results presented here significantly broaden the range of materials accessible by electrodeposition from supercritical fluid and open the future possibility to utilise the full scope of these unique fluids to electrodeposit functional binary or ternary alloys and compounds of the p-block.

[a] Professor P. N. Bartlett, Ms J. E. Burt, Dr D. A. Cook, Dr C. Y. Cummings, Ms M. M. Hasan, Professor A. L. Hector, Professor W. Levason, Dr D. Pugh, Professor G. Reid, Dr P. W. Richardson, Dr W. Zhang
Chemistry
University of Southampton
Highfield
Southampton SO17 1BJ, UK
E-mail: P.N.Bartlett@soton.ac.uk

[b] Professor M. W. George, Dr Je Kie, Ms N. Suleiman
School of Chemistry
University of Nottingham
University Park
Nottingham NG7 2RD, UK

[c] Professor M. W. George
Department of Chemical and Environmental Engineering
University of Nottingham Ningbo China
199 Talking East Road
Ningbo 315100, China

[d] Professor D. C. Smith, Mr J. Spencer
Physics and Astronomy
University of Southampton
Highfield
Southampton SO17 1BJ, UK.

Supporting information for this article is given via a link at the end of the document.

Introduction

Supercritical fluids (SCFs), that is fluids above their critical temperature and pressure, are characterised by their very low surface tension and viscosity, allowing them to penetrate the smallest nanopores irrespective of the nature of the pore wall. Combined with their low viscosity, and hence fast mass transport rate, this makes them uniquely well-suited for electrodeposition into high aspect ratio nanostructures. In previous work it has been shown to be possible to deposit extremely narrow, 3 nm diameter, copper nanowires via SCF electrodeposition,[1] i.e. at dimensions beyond those achieved using conventional electrochemical fluids, or other deposition methods. Further, depending on the choice of SCF, they can have high chemical stability and resistance to oxidation or reduction, giving wide potential limits[2] (more than 9 V depending on the choice of electrolyte). This could enable the deposition of a wide range of reactive materials and electrodeposition at elevated temperatures. Consequently, bringing together the long established advantages of electrodeposition with the use of supercritical fluids is a very attractive new approach to nanomaterials deposition. However, the low polarity of SCFs means that dissolving sufficient concentrations of ions in them (to form an electrolyte), coupled with the need to operate at elevated temperatures and pressures (to ensure sufficient fluid density while retaining a single phase), means that they are extremely challenging media from which to perform electrodeposition. While the electrodeposition of metallic copper and silver nanowires from supercritical fluids have been reported,[1],[3],[4] translation of this technique to deliver semiconducting or semi-metallic materials from the main group has proved very challenging.[5],[6] The main group elements feature strongly in semiconductor materials of key importance in modern electronic and optical devices, and this has provided the major impetus for us to develop the first general route for electrodeposition of a wide range of these elements (Ga, In, Ge, Sn, Sb, Bi, Se, Te) from supercritical difluoromethane under mutually compatible conditions. This is an important breakthrough that opens up the opportunity to use supercritical fluid electrodeposition to deposit extreme nanostructured devices.

As a materials deposition technology electrodeposition has a number of key distinguishing features: it is an additive process where the deposition is spatially localised and occurs directionally away from the electrode; it is a volume filling method without shrinkage; it is very efficient in its use of

material; it is controlled by the applied potential or current and so can be stopped and started at will and can be directly monitored during deposition. These features distinguish it from other widely used materials' deposition technologies. These features are exploited in the copper Damascene process pioneered by IBM and used to deposit electrical interconnects on VLSI silicon chips[7] and the commercial adoption of this process to replace aluminium interconnects by copper in integrated circuits has been essential to the progress of VLSI to its current level.

In electrodeposition the electrolyte (that is the combination of solvent and dissolved ions) plays a key role in determining what can be deposited. The majority of electrodeposition, from the Damascene copper process used in VLSI manufacture, to the deposition of copper vias on PCBs, and the electrodeposition of magnetic materials in read-write heads[8] uses aqueous solutions. Recently ionic liquids have been widely studied in electrochemistry and electrodeposition since they offer flexibility in the choice of solvent properties and a wide electrochemical window.[9],[10] However, significant challenges remain to achieve device quality semiconductor materials and the high viscosity and surface tension of ionic liquids means they are poorly suited to electrodeposition into extreme (sub 20 nm) nanostructures.

There are, however, significant technical challenges to overcome. The supercritical fluids that would be desirable to use for electrodeposition, because they are non-corrosive and have accessible critical temperatures and pressures, have low dielectric constants, typically below 10. Consequently, it can be difficult to achieve sufficient electrolyte solubility and ionic conductivity for good electrochemistry. As a result, in order to maximise solubility it is necessary to work under conditions where the density of the supercritical fluid remains above the critical density (typically around 80 to 90% of the density of the liquid). In addition, elevated pressures are required, so specialised equipment is necessary and experiments must be carried out in sealed, pressurised vessels. Nevertheless, progress has been made and the electrodeposition of copper and silver nanowires has been reported from supercritical CO_2 containing 13% acetonitrile as a co-solvent, as well as from supercritical difluoromethane, and the electrodeposition of germanium has been demonstrated.[1],[3-6]]

In this paper we report a significant advance in supercritical fluid electrodeposition that opens up a general route to the deposition of a number of p-block elements (Ga, In, Ge, Sn, Sb, Bi, Se, Te) from supercritical difluoromethane and thus very significantly widens the scope of the technique. An important feature of the electrolyte and the reagents employed in this work is that the components are mutually compatible, and therefore the results we report here pave the way for developing supercritical fluid electrodeposition towards binary and ternary semiconductor materials which are of key importance in modern electronic and optical devices, and as yet unknown for supercritical fluid electrodeposition (SCFED).

Results and Discussion

In order to successfully achieve SCFED of a wide range of p-block elements from scCH_2F_2, suitable (mutually compatible) reagents to provide the source of the elements and a supporting electrolyte need to be identified. For the reagents, key considerations are stability (mainly to oxygen and water) and solubility under supercritical conditions (T ~358 K, p ~17.2 MPa) in this low dielectric medium, as well as the ease of their electrochemical reduction. Some knowledge of speciation in the SCF is also very useful. We selected tetrabutylammonium chlorometallate salts since they are easily handled powders, can be prepared in high yields and exist for a wide range of the p-block elements, thus presenting the prospect that it will be possible to extend this system to enable deposition of binary and higher semiconductors and alloys through combining precursors in the SCF electrolyte. Previously we have described a range of different supporting electrolytes suitable for use in SCFED,[12],[13] the key criteria being high solubility and conductivity (dissociation into ions) in the very low dielectric SCF. Since it is expected that Cl^- will be liberated during reduction of the chlorometallate precursor, [N^nBu_4]Cl was identified as the most suitable supporting electrolyte, minimising the different types of ions present in the electrolyte system. Prior to its application in SCFED we therefore undertook a detailed study to determine the suitability of the electrolyte formed from [N^nBu_4]Cl in scCH_2F_2.

Phase Behaviour and Conductivity of [N^nBu_4]Cl in scCH_2F_2. A single, homogeneous fluid phase is the preferential condition to carry out electrodeposition in SCFs. To measure the solubility of [N^nBu_4]Cl in CH_2F_2, the p-T phase boundaries of 5 binary mixtures of [N^nBu_4]Cl + CH_2F_2 have been determined at temperatures between 293 and 373 K and pressures up to 15 MPa, see Figure 1(b). The relevant experimental data have been interpolated to T = 363 K. The resulting p-x phase diagram is shown in Figure 1(a). Clearly, when the temperature of the electrodeposition bath is 363 K, the minimum pressure required to dissolve 3.8×10^{-3} mole fraction (equivalent to approximately 0.06 mol dm^{-3} at 20 MPa and 363 K in CH_2F_2) is 9.6 MPa. Therefore, the electrodeposition conditions employed in this study were selected to ensure that [N^nBu_4]Cl is completely dissolved in CH_2F_2, see the hatched area in Figure 1(a).

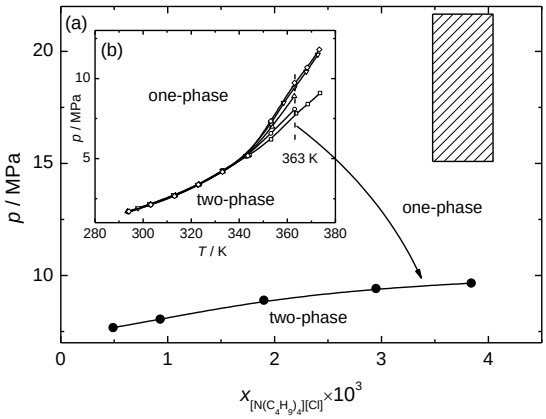

Figure 1. Phase diagrams of the binary mixture of $[N^nBu_4]Cl$ and CH_2F_2. (a) *p-x* diagram at 363 K, the hatched area represents the conditions (363 K, 15−22 MPa, and $x_{[N^nBu4]Cl}$ = (3.5−4.0)×10^{-3}) used in the electrodeposition. A solution of 0.060 mol dm^{-3} of $[N^nBu_4]Cl$ in CH_2F_2 is estimated to have a mole fraction of 3.8×10^{-3} at 363 K and 20 MPa. (b) *p*-T diagram for five mixtures with $x_{[N^nBu4]Cl}$ = 0.49×10^{-3} (□), 0.93×10^{-3} (○), 1.90×10^{-3} (△), 2.95×10^{-3} (▽) and 3.84×10^{-3} (◇).

Measurements of the electrical conductivity of 0.060 mol dm^{-3} of $[N^nBu_4]Cl$ in CH_2F_2 at 363 K (SI, Figure S2) showed that the conductivity increases with pressure exceeding ~2.0 mS cm^{-1} at ~14 MPa.

Electrochemistry of Tetrabutylammonium Chlorometallate Salts in scCH_2F_2/$[N^nBu_4]Cl$. The precursors, $[N^nBu_4][MCl_3]$ (M = Ge, Sn), $[N^nBu_4][MCl_4]$ (M = Ga, In, Sb, Bi) and $[N^nBu_4]_2[MCl_6]$ (M = Se, Te) were prepared using literature methods[13],[14] or slight modifications thereof, and their identities and purity established spectroscopically (IR, Raman, ^{119}Sn, ^{71}Ga, ^{115}In, ^{77}Se and ^{125}Te NMR) and by microanalysis.

The voltammetric characteristics of all eight of the p-block precursors at 17.2 MPa and 358 K are presented in Figure 2. The grey scans included in each of the figures correspond to the voltammetric response measured in the pure $[N^nBu_4]Cl$ supporting electrolyte in scCH_2F_2, and establishes the potential window available in this system. The current density in the voltammogram of the supporting electrolyte does not exceed 3 mA cm^{-2} between −2.0 and 1.0 V, indicating that the electrolyte provides a wide potential window. Figure 2 also shows that fluctuations are observed at cathodic potentials in the limiting current density region of all eight voltammograms of the redox species. Fluctuations such as these often occur for voltammetry in SCFs and it has been shown that they are due to the effects of convection in the cell caused by temperature gradients, which are exacerbated by the low viscosity of the SCF.[15]

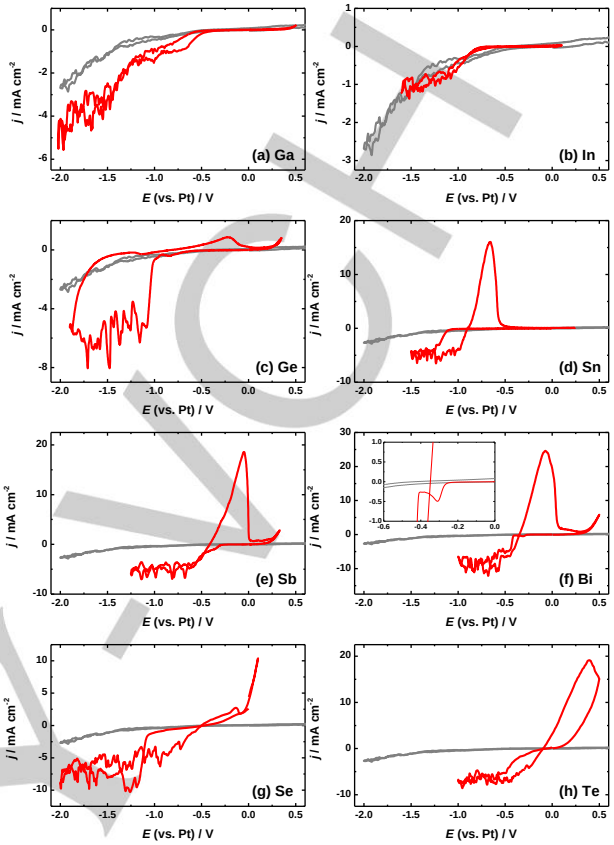

Figure 2. Cyclic voltammograms of (a) $[N^nBu_4][GaCl_4]$, (b) $[N^nBu_4][InCl_4]$, (c) $[N^nBu_4][GeCl_3]$, (d) $[N^nBu_4][SnCl_3]$, (e) $[N^nBu_4][SbCl_4]$, (f) $[N^nBu_4][BiCl_4]$, (g) $[N^nBu_4]_2[SeCl_6]$, (h) $[N^nBu_4]_2[TeCl_6]$ in sc-CH_2F_2 (17.2 MPa and 358 K) measured on 1.0 or 0.5 mm gold working electrodes and referenced to a Pt pseudo-reference electrode. The concentration of the $[N^nBu_4]_x[MCl_y]$ redox species in each case was 2×10^{-3} mol dm^{-3}, with the exception of the $[N^nBu_4][InCl_4]$ which used 0.4×10^{-3} mol dm^{-3}. 50×10^{-3} mol dm^{-3} $[N^nBu_4]Cl$ was used as the supporting electrolyte. The potential scan rate was 50 mV s^{-1}. The grey scans included in each of the figures correspond to the voltammetric response measured in the pure $[N^nBu_4]Cl$ supporting electrolyte in scCH_2F_2.

Ga and In. The voltammetry for $[N^nBu_4][GaCl_4]$ is presented in Figure 2(a). Two irreversible cathodic waves are observed at −0.50 V and −1.34 V. The magnitude of the wave heights relative to each other (i.e. 1:2) suggests that the first wave may correspond to the reduction of Ga(III) to Ga(II), while we attribute the second to the reduction of Ga(II) to Ga(0) metal. Isolated mononuclear Ga(II) compounds are rare, although Ga(II) species are known to persist in solution and the thermodynamic and kinetic parameters for Ga(II) *vs.* Ga(I) and Ga(III), are a delicate balance in a specific chemical environment.[16] For Ga there is no stripping peak on the reverse anodic scan.

Figure 2(b) shows the voltammetry of the $[N^nBu_4][InCl_4]$ precursor. The current density observed for this complex is significantly smaller (approx. $^1/_{10}$) than for the other compounds. It is most likely that this is due to the lower solubility of the In(III) precursor salt in solution. Previous ^{115}In NMR studies on a solution of $[N^nBu_4][InCl_4]$ in CH_2Cl_2 solution in the presence of a 10-fold excess of $[N^nBu_4]Cl$ showed that $[InCl_6]^{3-}$ is the major species present (13). It is reasonable to assume that similar speciation occurs in $scCH_2F_2$, and the trianionic $[InCl_6]^{3-}$ would be expected to have much lower solubility in the low dielectric SCF. It was therefore necessary to use reduced concentrations of the $[N^nBu_4][InCl_4]$ in the plating bath to achieve satisfactory electrochemical behaviour. The voltammogram shows an irreversible reduction wave with an onset at about –0.70 V. No stripping peak is observed on the anodic scan. When the experiments were repeated in $[N^nBu_4][BF_4]$ background electrolyte the voltammetry showed a single reduction wave and stripping peak and ^{115}In NMR spectroscopy confirms that the species in this solution is $[InCl_4]^-$ (+446 ppm, see SI). The reduction wave was mass transport limited with an onset at about -1.10 V with a steady state current density of ~6 mA cm^{-2} (see SI). This current density is comparable to that for the other complexes in Figure 2 suggesting that in the absence of excess chloride the $[InCl_4]^-$ is soluble in the supercritical fluid.

Ge and Sn. The voltammogram of the $[N^nBu_4][GeCl_3]$ complex (Figure 2(c)) is characterised by a steep cathodic wave with an onset potential of approximately –1.0 V, and an erratic limiting current that extends to –1.9 V. Following the reversal of the scan direction, the current density decays to zero, indicating that the reduction of the Ge(II) to Ge(0) species is inhibited. An anodic stripping peak with an onset potential of approximately –0.50 V is also observed. There is a large discrepancy between the charge densities associated with the deposition and stripping peaks. While the total reduction charge is 1.17 mC cm^{-2}, the stripping charge is 0.013 mC cm^{-2}.

Figure 2(d) shows the voltammetry for $[N^nBu_4][SnCl_3]$. The voltammogram shows typical metal deposition and stripping features with a well-characterised nucleation loop and stripping peak. The onset of nucleation occurs at approximately –1.10 V and the stripping onset at about –0.90 V. The charge density associated with the deposition and stripping reactions is 0.81 mC cm^{-2} and 0.58 mC cm^{-2}, respectively. The Faradaic efficiency is ~70%.

Sb and Bi. The cyclic voltammetry for $[N^nBu_4][SbCl_4]$ is presented in Figure 2(e). The deposition onset of the Sb reduction is approximately –0.32 V. A current plateau is observed in the anodic scan until the stripping onset occurs at about –0.42 V. The total reduction charge for the Sb is 1.49 mC cm^{-2} and the stripping charge is 0.74 mC cm^{-2}, with a Faradaic efficiency of 50%. The cyclic voltammetry of the $[N^nBu_4][BiCl_4]$ complex presented in Figure 2(f) shows a well-defined nucleation loop and stripping peak. The deposition onset and stripping onset are at –0.41 V and –0.35 V respectively. A small cathodic peak at –0.31 V observed prior to the onset of Bi reduction (see inset in Figure 2f) is attributed to the under potential deposition (UPD) of Bi. The charge associated with this peak corresponds to the adsorption of a monolayer of Bi on the surface of the gold electrode. The Faradaic efficiency of the Bi deposition is 64%, with a deposition charge of 1.85 mC cm^{-2} and a stripping charge of 1.18 mC cm^{-2}.

Se and Te. The deposition voltammetry for the $[N^nBu_4]_2[SeCl_6]$ is presented in Figure 2(g). The voltammogram shows an irreversible reduction wave with an onset potential of about –1.0 V and a peak deposition current density at –1.25 V. There is a small stripping peak on the reverse anodic scan at about -0.13 V, which occurs immediately before the onset of chloride oxidation at 0.00 V.

The voltammetry of the $[N^nBu_4]_2[TeCl_6]$ is presented in Figure 2(h). This shows the typical nucleation loop and stripping peak expected for metal deposition. The deposition onset potential is approximately –0.25 V and the stripping onset is –0.10 V. The stripping peak at 0.4 V is truncated by the reversal of the anodic scan direction at 0.5 V. This is necessary as the peak becomes convoluted with chloride oxidation at potentials positive to 0.5 V. The charge associated with the Te deposition and stripping is 1.79 mC cm^{-2} and 1.77 mC cm^{-2}, respectively, yielding a high Faradaic efficiency of 99%.

Additional voltammetry studies of the Se and Te complexes, at Pt and TiN electrodes, have shown that the onset of chloride oxidation shifts to more positive potentials for both elements on these other substrate materials (see SI for details).

SCFED of p-block Elements. The p-block elements were electrodeposited potentiostatically from $scCH_2F_2$ onto evaporated gold slide electrodes. All elements were deposited at constant potential, with the deposition potentials and times specifically selected for each element in order to obtain films of sufficient thickness for EDX and XRD analyses (1 to 2 μm), as detailed in Table 1. After depressurisation, the electrodes with the deposited films were removed from the cell (for Ge, In, Sb this was done inside a nitrogen-purged glovebox) and then gently washed by dipping into CH_2Cl_2 solution to dissolve away residual electrolyte salts. The deposited films were analysed by SEM, EDX and XRD.

Table 1. Electrodeposition parameters for all p-block elements deposited onto Au electrodes. Concentration of all precursor compounds was 2×10^{-3} mol dm^{-3}, except for $[InCl_4^-]$ which was 0.4×10^{-3} mol dm^{-3}, with 50×10^{-3} mol dm^{-3} $[N^nBu_4]Cl$ used as the supporting electrolyte. Pressure = 17.2 MPa, temperature = 358 K.

Element	Deposition potential / V *vs*. Pt	Deposition time / s	Charge passed / C
Ga	-2.00	5500	1.31
In	-1.50	6828	2.65
Ge	-1.80	5497	1.39
Sn	-1.25	1001	1.30
Sb	-0.75	8000	0.42
Te	-0.80	3501	4.00
Bi	-0.90	1034	1.14
Se	-1.25	3600	0.64

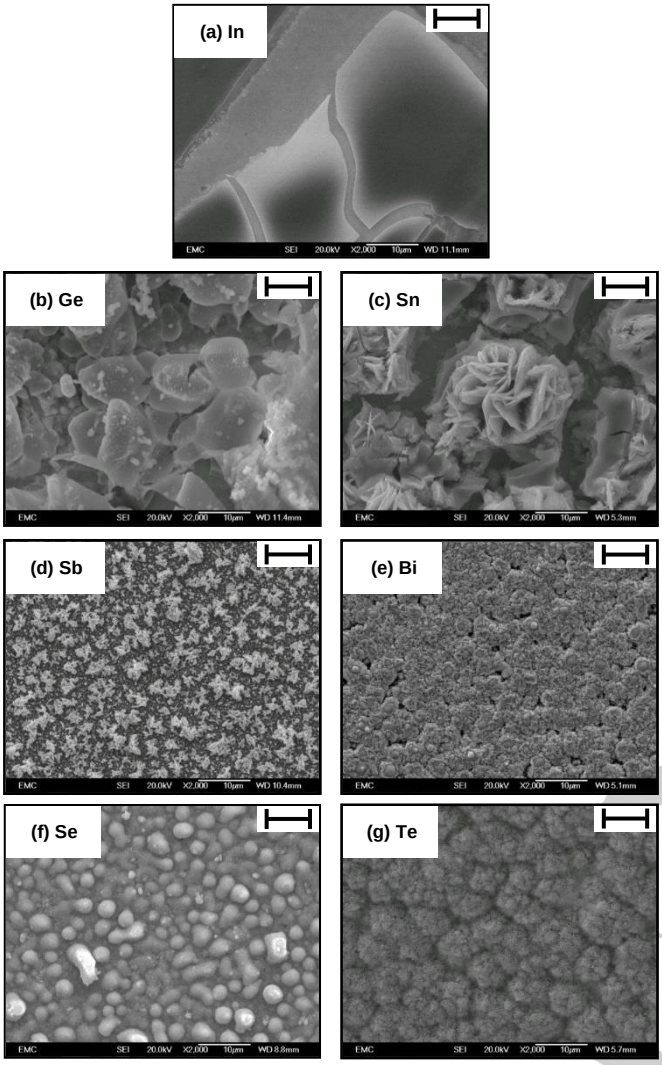

Figure 3. SEM images of electrodeposited films of (a) In, (b) Ge, (c) Sn, (d) Sb, (e) Bi, (f) Se and (g) Te on evaporated gold slide electrodes. The scale bars represent 10 μm. The deposition conditions are given in Table 1.

SEM images (Figure 3) show that, in general, the materials have quite uniform morphologies across the electrode surface and that the film adhesion on Au was generally good. The exceptions were the Ga which was liquid as deposited and hence the small droplets of elemental Ga readily detached from the electrode surface, and the Se which almost entirely detached from the electrode surface upon washing in the CH_2Cl_2 solvent. The SEM imaging shows that the Se material that remained on the electrode has a relatively smooth morphology with micro-grains of < 1 μm in length. For the Sn, Sb, Te and Bi samples, the crystalline facets are clearly visible in the images, whereas the electrodeposited In forms smoother thin layers which tend to roll up. The Ge film is also quite smooth, and shows good coverage across the electrode surface. The EDX spectra of the deposited films are shown in the SI (Figure S3). In each case, the target element was observed as the dominant peaks, with peaks from the Au substrate also evident in some cases. Negligible Cl was observed by EDX on samples after washing in CH_2Cl_2, suggesting that this procedure was highly effective at removal of electrolyte salts.

XRD measurements were undertaken to confirm the structures of the materials electrodeposited on gold electrodes, with the exception of Ga (a liquid) and Se, where there were problems with adhesion. In the case of Sb and Te XRD provided evidence of alloying with the gold. Hence Sb, Se and Te samples were also deposited on TiN. Representative XRD patterns are presented in Figure 4, and are consistent with previously reported data for the bulk elements, except for Ge, which is almost amorphous as-deposited but can be crystallised at 700 ºC (see SI). The experimental and literature data are presented in Table 2.

Table 2. Refined parameters from the XRD patterns in Figure 4.

Element	Crystal structure : Space group	Lattice parameters /Å	Literature lattice parameters	Crystallite size / nm
In	Tetragonal: I4/m m m (139)	a = 3.2411(5) c = 4.9286(9)	a = 3.2520(2) c = 4.9466(2) [17]	22
Sn	Tetragonal: I 4_1/a m d S (141)	a = 5.8558(7) c = 3.1966(5)	a = 5.8317(2) c = 3.1813(2) [18]	76
Bi	Trigonal: R -3 m H (166)	a = 4.5394(19) c = 11.834(9)	a = 4.535(2) c = 11.814(6) [19]	15
Te	Hexagonal: P$3_1$21 (152)	a = 4.4366(15) c = 5.9040(7)	a = 4.456(1) c = 5.921(2) [20]	38
Sb on TiN	Trigonal: R -3 m H (166)	a = 4.311(3) c = 11.324(15)	a = 4.3084(2) c = 11.274(6) [21]	56
Se on TiN	Hexagonal: P$3_1$21 (152)	a = 4.389(4) c = 4.970(7)	a = 4.368(3) c = 4.958(4) [22]	19
Te on TiN	Hexagonal: P$3_1$21 (152)	a = 4.4846(11) c = 5.9568(10)	a = 4.456(1) c = 5.921(2) [20]	39

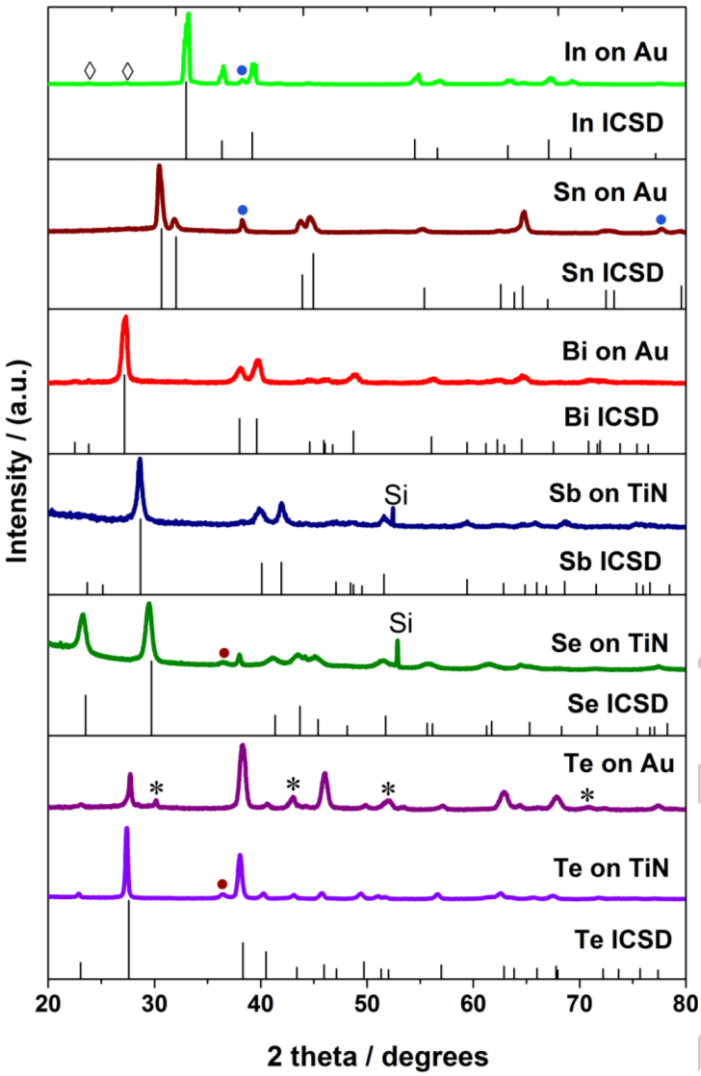

Figure 4. Grazing incidence diffraction patterns (1° incidence angle) for In, Sn, Bi, Sb, Se and Te deposited on gold and TiN. * marks the positions of peaks due to $Au_{0.3}Te_{0.7}$ alloy, and ◊ marks the positions of $AuIn_2$ peaks. • marks Au and • marks the TiN peaks. Comparison patterns come from the Inorganic Crystal Structure Database (ICSD).[23] All samples were deposited from plating solutions containing 2×10^{-3} mol dm^{-3} chlorometallate with 50×10^{-3} mol dm^{-3} $[N^nBu_4]Cl$ except for In where the electrolyte was 50×10^{-3} mol dm^{-3} $[N^nBu_4][BF_4]$.

The diffraction data from the electrodeposited In sample confirmed that elemental In was indeed present, although the sample was very thin, hence the diffraction pattern was dominated by peaks from the Au substrate. The pattern shown in Figure 4 was for a sample deposited from $[N^nBu_4][BF_4]$ electrolyte to improve the solubility and allow deposition of a thicker film (see SI for details). The resultant films have no preferred orientation. Tetragonal Sn samples grown by SCFED showed elongation of the Sn 200 reflection relative to the intensity distribution from the literature XRD pattern.[18] Symmetric (θ-2θ) XRD scans confirmed some <200> preferred orientation. This is a common feature of electrodeposition processes, but in this case could also be related to the strong <111> alignment of the sputtered gold electrode surfaces. The electrodeposited antimony on gold showed the presence of Sb but also significant amounts of $AuSb_2$ (*Pa*-3, *a* = 6.63497(16) Å), the latter clearly formed by alloying with the gold electrode surface. Deposition on TiN resulted in phase pure Sb with no evidence of alloying or preferred orientation. Bi deposits showed a normal XRD intensity distribution, consistent with polycrystalline Bi on gold. As remarked above, Se adhesion on gold was poor, however electrodeposition on TiN gave good adhesion and the resulting Se films were polycrystalline. Alloying was less significant, but still present, in Te electrodeposition on gold, with visible diffraction peaks consistent with cubic $Au_{0.3}Te_{0.7}$ (*Pm*-3*m*, *a* = 2.9682(13) Å). The symmetric scans also showed clearly that the film had strong <001> preferred orientation due to the enhancement of the 003 reflection. Films deposited on TiN were phase pure Te with no evidence of any alignment. Raman spectra from samples of Se, Sb, Te and Bi (see SI) confirm the presence of the XRD identified crystalline form of the relevant element. In the case of Ge Raman spectra for as deposited samples is consistent with amorphous Ge (see SI) and Raman spectra on annealed material confirm the presence of crystalline Ge. The other materials are not significantly Raman active.

Conclusions

In this paper we have described a common approach to the electrodeposition a range of p-block elements from supercritical difluoromethane by using the chlorometallate complexes in an electrolyte of tetrabutylammonium chloride. We have shown that under the deposition conditions, 50×10^{-3} mol dm^{-3} $[N^nBu_4]Cl$ at 17.2 MPa and 358 K, the system is a single, supercritical phase well away from the phase boundary and that the electrolyte has sufficient conductivity to be used for electrodeposition. The electrolyte has a stable 3 V potential window that extends to around −2.0 V *vs*. Pt. In each case, voltammetry of the complexes at gold electrodes shows clear reduction waves for deposition of the element.

Using this approach we have demonstrated the deposition of elemental Ga, In, Ge, Sn, Sb, Bi, Se, Te. In all cases, with the exception of Ga, which is a liquid under the deposition conditions, the resulting deposits on gold or TiN were characterised by scanning electron microscopy, energy dispersive X-ray analysis, X-ray diffraction and, for Ge, Sb, Bi, Se and Te, Raman spectroscopy.

By using the anionic ($[GaCl_4]^-$, $[InCl_4]^-$, $[GeCl_3]^-$, $[SnCl_3]^-$, $[SbCl_4]^-$, and $[BiCl_4]^-$) and dianionic ($[SeCl_6]^{2-}$ and $[TeCl_6]^{2-}$) chlorometallates of the elements as their tetrabutylammonium salts, we demonstrate a compatible electrolyte system that can be used for these different elements. An advantage of these reagents is that they are all crystalline solids that are reasonably easy to handle and that are not highly water or oxygen sensitive.

The results presented here significantly broaden the range of materials accessible by electrodeposition from supercritical fluid and open the future possibility to exploit all of the advantages of these unusual fluids to deposit binary or ternary alloys and compounds of the p-block.

Experimental Section

Reagents. All reagents were handled under rigorously anhydrous conditions via a dry dinitrogen atmosphere and standard Schlenk and glove-box techniques. Anhydrous $[N^nBu_4]Cl$ was obtained from Sigma and used as received. $[N^nBu_4][BF_4]$ was obtained Sigma Aldrich (≥99.0% grade) and dried for 2 h at 100 °C under vacuum before use. Tetra-*n*-butylammonium chlorometallate salts were made by the literature methods[13],[14] or as described in the Supporting Information. Difluoromethane was supplied by Apollo Scientific Ltd UK with a purity of 99.9 wt/wt%.

Phase Equilibrium Measurements. The phase equilibrium of the binary mixture of $[N^nBu_4]Cl + CH_2F_2$ was studied by using a so-called synthetic approach.[24] The synthetic approach required that the equilibrium vessel was first loaded with the $[N^nBu_4]Cl + CH_2F_2$ mixture of a known composition (e.g. the mole fraction of $[N^nBu_4]Cl$). The phase boundary was determined by the observation of the phase transition when varying temperature, or pressure or both. The experiments were conducted in a variable-volume view cell, the detailed description of which can be found in the literature.[25]

Electrochemical Measurements. Supercritical fluid electrochemical studies were performed in a stainless steel high-pressure cell, the details of which have been described in previous publications (10, 25). The dry powdered reagents and electrolyte complexes (i.e. $[N^nBu_4]_x[MCl_y]$ and $[N^nBu_4]Cl$) were transferred into the cell inside a nitrogen-purged glove box (Belle Technology). All electrolytes were prepared with 2×10^{-3} mol dm^{-3} of the $[N^nBu_4]_x[MCl_y]$ as the redox species and 50×10^{-3} mol dm^{-3} of the $[N^nBu_4]Cl$ as the supporting electrolyte, with the exception of the $[N^nBu_4][InCl_4]$ which used 0.4×10^{-3} mol dm^{-3} of the redox species. Once sealed, the cell was removed from the glove box, connected to a high-pressure rig and heated to the desired temperature using a band heater under PID (proportional-integral-derivative) control. The $scCH_2F_2$ was then introduced using a specialised carbon dioxide pump (PU-1580-CO_2, JASCO) until the desired pressure was achieved. To ensure that the solution was homogeneous, the system was stirred during pumping using a magnetic stirrer. Stirring was stopped at least 5 min prior to electrochemical measurements. All experiments were carried out at 17.2 MPa and 358 K.

The electrochemical experiments were performed using a three-electrode system. A platinum mesh was used as the counter electrode, and a 0.5 mm diameter platinum disk was used as a pseudo-reference electrode. Gold disks of 1.0 or 0.5 mm diameter, polished to a mirror finish with alumina paste (1.0 and 0.3 μm) on microfiber polishing cloth (Buehler), were used as the working electrodes for voltammetric characterisation of the compounds. Cyclic voltammetry measurements were recorded at potential sweep rates of 50 mV s^{-1}. Films were electrodeposited potentiostatically onto evaporated gold slides that consisted of microscope slides with a 5 nm chromium adhesion layer and 100 nm of gold. Prior to electrochemical experiments, the gold slides were cleaned by ultrasonic agitation in isopropanol for 10 min and then dried under flowing argon. TiN electrodes were fabricated from commercial wafers of high resistivity, intrinsic silicon (<100> orientation, 380 μm thick) coated with a 300 nm layer of PVD deposited TiN which was coated with a 100-200 nm thick layer of PECVD deposited silicon dioxide (Si-Mat GmbH). To prepare as electrodes the wafers were first coated with a 500 nm layer of MMA resist to protect the surface, then diced into ~7.5 mm or 10 mm squares. The protective MMA resist was removed by cleaning in acetone (2.5 min) and IPA (2.5 min). The square pieces were then etched in buffered HF for 50 s to remove the silicon dioxide capping layer. The resistance of the TiN electrodes was measured to be 40-45 Ω. Electrodes were contacted to PEEK sealed stainless steel feedthroughs using silver epoxy (Eccobond 60L, Hitek Electronic Materials LTD, UK). The exposed stainless steel and silver epoxy was insulated against contact with the supercritical fluid using Struers EpoFix epoxy.

Characterisation of Electrodeposited Materials. All deposits were held in a static a solution of CH_2Cl_2 for 1 min after electrodeposition to wash them. The deposited films were investigated using scanning electron microscopy (SEM), energy dispersive X-ray (EDX) analysis, X-ray diffraction (XRD) and Raman spectroscopy as appropriate. A Jeol JSM 6500F field emission gun scanning electron microscope (FEG-SEM) equipped with an Oxford Instruments EDX detector were used for the SEM and EDX analyses, with accelerating voltage = 20 keV. XRD patterns were collected with a Rigaku Smartlab Thin Film (9 kW) diffractometer using a 0.1 mm parallel X-ray beam (Cu-K_α) and DTex250 1D detector. Grazing incidence patterns were collected with a 1° incident angle, and symmetric (θ-2θ) scans were used to examine preferred orientation. Data collections used either 2 or 0.5 mm length limiting slit, depending on sample size. Crystallite size calculations used data from a LaB_6 standard previously collected under the same conditions to model the instrumental peak shape. Data were modelled using the Rigaku PDXL2 package with patterns from the JCPDS database.[26]

Raman spectroscopy was performed using a Coherent MIRA-900 Ti:Sapphire laser source in CW mode set to 702 nm and filtered using a Photonetc TLS 850 laser line filter. Raman spectra were taken in a back scattering geometry using an Olympus LMPan IR 50x objective with a power density of 2 MW/μm^2 on the sample. Back scattered light was collected into a Princeton Instruments TriVista triple 600 nm spectrometer, configured in subtractive mode, using 900, 900 and 1800 lines/mm gratings in three stages. Spectra was measured on a Princeton Instruments, deep depleted, liquid N_2-cooled silicon CCD.

Acknowledgements

We thank EPSRC for a Programme Grant (EP/I033394/1) and for support for XRD (EP/K00509X and EP/K009877/1). The SCFED Project (www.scfed.net) is a multidisciplinary collaboration of British universities investigating the fundamental and applied aspects of supercritical fluids. PNB acknowledges receipt of a Wolfson Research Merit Award.

Supporting Information

Synthetic procedures for chlorometallate precursors; conductivity measurements; Raman spectra where relevant; EDX data for each element: additional voltammetry; XRD data for electrodeposited films. These data may be accessed via XXXXX.

Keywords: supercritical fluid • electrodeposition • main group • p-block

[1] J. Ke, W. Su, S. M. Howdle, M. W. George, D. Cook, M. Perdjon-Abel, P. N. Bartlett, W. Zhang, F. Cheng, W. Levason, G. Reid, J. Hyde, J. Wilson, D. C. Smith, K. Mallik, P. Sazio, *Proc. Natl. Acad. Sci., USA* 2009, **106**, 14768-14772.

[2] A. P. Abbott, C. A. Eardley, J. C, Harper, E. G. Hope, *J. Electroanal. Chem.* 1998, **457**, 1-4.

[3] D. Cook, P. N. Bartlett, W. Zhang, W. Levason, G. Reid, J. Ke, W. Su, M. W. George, J. Wilson, D. Smith, K. Mallik, E. Barrett, P. Sazio, *Phys. Chem. Chem. Phys.* 2010, **12**, 11744-11752.

[4] P. N. Bartlett, M. Perdjon-Abel, D. Cook, G. Reid, W. Levason, F. Cheng, W. Zhang, M. W. George, J. Ke, R. Beanland, J. Sloan, *ChemElectroChem*, 2014, **1**, 187-194.

[5] J. Ke, P. N. Bartlett, D. Cook, T. L. Easun, M. W. George, W. Levason, G. Reid, D. Smith, W. Su, W. Zhang, *Phys. Chem. Chem. Phys.* 2012, **14**, 1517-1528.

[6] P. N. Bartlett, D. A. Cook, M. W. George, A. L. Hector, J. Ke, W. Levason, G. Reid, D. Smith, W. Zhang, *Phys. Chem. Chem. Phys.* 2014, **16**, 9202-9219.

[7] P. C. Andricacos, C. Uzoh, J. O Dukovic, J. Horkans, H. Deligianni, *IBM J. Res. and Dev.* 1991, **42**, 567-574.

[8] E. I. Cooper, C. Bonhôte, J. Heidmann, Y. Hsu, P. Kern, J. W. Lam, M. Ramasubramanian, N. Robertson, L. T. Romankiw, and H. Xu, *IBM J. Res. & Dev.* 2005, **49**, 103-126.

[9] H. Liu, Y. Liu, J. Li, *Phys. Chem. Chem. Phys.* 2010, **12**, 1685-1697.

[10] F. Endres, D. MacFarlane, A. Abbott (Eds) *Electrodeposition from Ionic Liquids*, Wiley, Chichester 2008.

[11] P. N. Bartlett, D. Cook, M. W. George, J. Ke, W. Levason, G. Reid, W. Su, W. Zhang, *Phys. Chem. Chem. Phys.* 2011, **13**, 190-198.

[12] P. N. Bartlett, D. Cook, M. W. George, J. Ke, W. Levason, G. Reid, W. Su, W. Zhang, *Phys. Chem. Chem. Phys.* 2010, **12**, 492-501.

[13] C. D. Schmulbach, I. Y. Ahmed, *Inorg. Chem.* 1971, **10**, 1902-1907.

[14] P. N. Bartlett, D. A. Cook, C. H. de Groot, A. L. Hector, R. Huang, A. Jolleys, G. P. Kissling, W. Levason, S. Pearce, G. Reid, *RSC Advances* 2013, **3**, 15645-15654.

[15] J. A. Branch, D. A. Cook, P. N. Bartlett, *Phys. Chem. Chem. Phys.* 2015, **17**, 261-267.

[16] M. J. Taylor, P. J. Brothers, *Chemistry of Aluminium, Gallium, Indium and Thallium*, ed A. J. Downs, Blackie, London, 1993, Ch. 3.

[17] M. Wolcyrz, R. Kubiak, S. Maciejewski, *Phys. Stat. Solidi. B - Basic Sol. St. Phys.* 1981, **107**, 245-253.

[18] J. A. Lee, G. V. Raynor, *Proc. Phys. Soc. London* 1954, **67**, 737-747.

[19] P. Cucka, C. S. Barrett, *Acta Crystallogr.* 1962, **15**, 865-872.

[20] C. Adenis, V. Langer, O. Lindqvist, *Acta Crystall., Sect. C* 1989, **45**, 941-942.

[21] C. S. Barrett, P. Cucka, K. Haefner, *Acta Crystall.* 1963, **16**, 451-453.

[22] R. Keller, W. B. Holzapfel, H. Schulz, *Phys. Rev, Ser. 3: Solid State* 1977, **16**, 4404-4412.

[23] ICSD, *accessed via the EPSRC-funded National Chemical Database Service hosted by the Royal Society of Chemistry*.

[24] R. Dohrn, G. Brunner, *Fluid Phase Equilibria* 1995, **106**, 213-282.

[25] P. Licence, M. P. Dellar, R. G. M.Wilson, P. A. Fields, D. Litchfield, H. M. Woods, M. Poliakoff, S. M. Howdle, *Rev. Sci. Instrum.*, 2004, **75**, 3233–3236.

[26] *PDF-2 Powder Diffraction File, 2004 release,* International Center for Diffraction Data, Swarthmore, PA.

Entry for the Table of Contents (Please choose one layout)

Layout 1:

FULL PAPER

Compatible conditions: electrodeposition of a range of p-block elements under compatible conditions from supercritical difluoromethane opens up the possibility to electrodeposit sub 20 nm nanostructures of a wide range of p-block binary and ternary alloys and compounds.

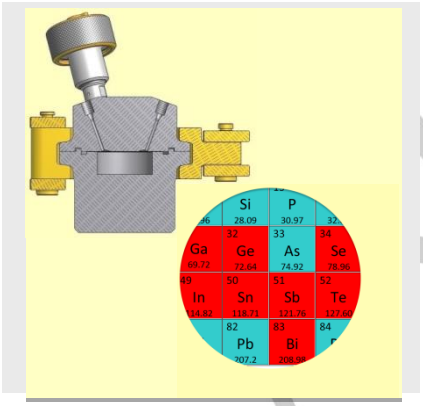

Philip N. Bartlett, Jennifer Burt, David A. Cook, Charles Y. Cummings, Michael W. George, Andrew L. Hector, Mahboba M. Hasan, Jie Ke, William Levason, David Pugh, Gillian Reid,Peter W. Richardson, David C. Smith, Joe Spencer, Norhidayah Suleiman, Wenjian Zhang*

Page No. – Page No.

A Versatile Precursor System for Supercritical Fluid Electrodeposition of Main Group Materials